

doi: 10.18720/MCE.83.2

## Stress-strain state of a steel-reinforced concrete slab under long-term

## Напряженно-деформированное состояние сталежелезобетонной плиты при длительных нагружениях

*F.S. Zamaliev\**,  
*M.A. Zakirov*,  
Kazan State University of Architecture and  
Engineering, Kazan, Russia

*Канд. техн. наук, доцент Ф.С. Замалиев\**,  
*аспирант М.А. Закиров*,  
Казанский государственный архитектурно-  
строительный университет, г. Казань,  
Россия

**Key words:** steel reinforced concrete slab; numerical experiments; full-scale tests; stresses; deflections; comparisons

**Ключевые слова:** сталежелезобетонная плита; численные эксперименты; натурные испытания; напряжения; прогибы; сравнения

**Abstract.** This article explores the evaluation of the stress-strain state of steel reinforced concrete slabs under the action of long-term loads. The technique of computer simulation for the performance evaluation of steel reinforced concrete slabs under short-term and long-term loads and the results of numerical studies are shown. A unit for long-term tests has been prepared based upon the numerical studies. The mounting locations of instruments for measuring vertical displacements, the label diagram of sensors of strains in steel reinforced concrete test structures are given. The measurement results are summarized in tables and graphs. The analysis of the results of full-scale tests is given as are comparisons with numerical experiments' data. Analytical expressions for the calculation of steel reinforced concrete slabs for long-term loads taking into account the creep of concrete are given.

**Аннотация.** Оценке напряженно-деформированного состояния сталежелезобетонной плиты при действии длительных нагрузок посвящена данная статья. Приведены методика компьютерного моделирования оценки работы составной плиты при кратковременных и длительных нагружениях, результаты численных исследований. На основе численных исследований подготовлена установка для длительных испытаний. Приведены места установки приборов для замера вертикальных перемещений схема наклейки датчиков деформаций бетона и стали на испытываемой конструкции. Результаты измерений сведены в таблицы и графики. Дан анализ результатов натурных испытаний и сравнения с данными численных экспериментов. Приведены также аналитические выражения для расчета сталежелезобетонных плит на длительные нагружения с учетом ползучести бетона.

### 1. Introduction

In recent years, the construction practice has exhibited a tendency of expanding the application of steel reinforced concrete structures which renders their further study more relevant. However, the studies of steel reinforced concrete flexible elements are mainly dedicated to the identification of the stress-strain state by short-term external impacts [1–18] or to the identification of their preoperational stress-strain state [19–20]. To study the stress-strain state of steel reinforced concrete structures both analytical [1–8] and experimental methods – that is numerical experiments [14–18], or full-scale tests [19–20] are employed. The article deals with studies of steel reinforced concrete slabs for the action of long-term loads. The applicable Eurocode in European countries and the Russian design and construction specifications SP 266.1325800.2016 mainly view steel reinforced concrete structures under the action of short-term loads.

In order to identify the stress-strain state of steel reinforced concrete structures, different mathematical models and experimental studies on large-scale field models are employed. Experimental studies on full-scale models require considerable time, human and physical costs. Therefore, it is quite often that mathematical models which lead to faster results are selected. Many researchers while in search of effective mathematical models come to use numerical experiments based on application software. However, the accuracy of the data in large part depends on the proper choice of the numerical experiment model that would correspond to the physical operational essence of the nature structure by all the

parameters. There are many PC software systems (SCAD, Microfe, LIRA, ANSYS, etc.) used by researchers to model the elements of building structures. When choosing a PC, the question arises as to how close they are to the actual operation of the structures and how accurately they can assess the behavior of the structural element from its zero load up to the point of its destruction as well as taking into account the stress-strain state in various modes of load (short-term, long-term, repeated-static loads).

Studies of steel reinforced concrete structures on the basis of a mathematical model using application programs with further verification of the calculation results is an actual task. In this connection, the following tasks are set:

- The choice of the settlement complex, most fully reflect the actual work of the composite slab under operating loads.
- Analysis of the stress-strain state of the slab under the operational load (stresses in the ribs and plate, deflections, shear at the "steel-concrete" boundary)
- Carrying out full-scale tests of the model of composite slab on a scale of 1: 2.
- Comparison of results of full-scale tests with analogous data of numerical studies.
- Record analytical expressions for the evaluation of strength for the case of prolonged loading and comparison of calculation results by analytical formulas with the data of numerical and on-line experiments.

## 2. Methods and Results

The third stage (post-processing) is the analysis of calculation results. The calculated physical quantities (displacements, strains, stress, temperature and others) are represented in the ANSYS graphic window as pictures, tables, diagrams, animations.

The following structural solution was studied:

The steel part of the steel-concrete composite slab is the 3 000 mm rolled I-beams #14 per; the dimensions of the heavy B25 concrete slab part are as follows: length is 3 000 mm, width is 3 000 mm, height is 45 mm (Figure 1).

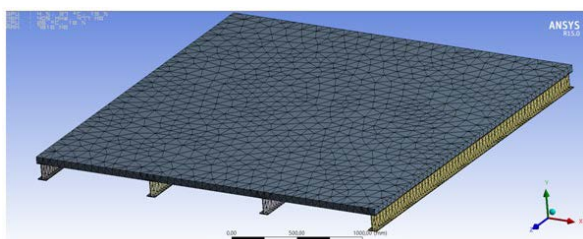


**Figure 1. Finite-element mesh generation of the steel-concrete composite slab**

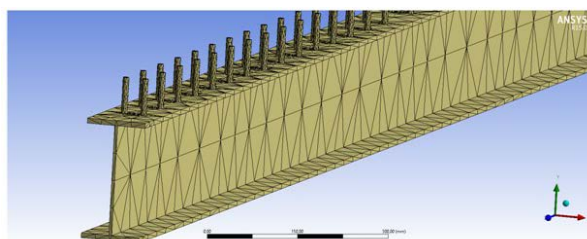


**Figure 2. Finite-element mesh generation of the I-beam**

The anchors are made from steel reinforcement in the form of two rows of 60 mm tall vertical bars ( $2\phi 8$  S245), welded throughout the entire length to the upper flange of steel beams spaced at intervals of 150 mm in the middle of the stairwell and of 100 mm on the ends (Figure 2). Height of the full construction is 190 mm.

The next stage of modelling is to select materials for the created bodies and to specify their properties.

For these purposes, there is a separate material management unit in Workbench, which deals with the analysis unit and is represented by the Engineering Data unit. For this particular slab, two materials from the library of General Materials – the library of the general use materials – were used; however, some characteristics were altered.

Metal ductility is calculated via a non-linear material model. In this particular case, Bilinear Isotropic Hardening was selected from the plasticity models.

For obtaining the numerical solution, it is necessary to split the geometric models by the finite-element grid. This procedure is carried out in the Modelling unit "Mechanical". The grid on solid bodies is created with the aid of the tetrahedral or hexahedral solid-state members. For this particular slab, the Medium grid – from  $75^\circ$  to  $24^\circ$  – was used in the Relevance center. There also exists a Fine grid – from  $36^\circ$  to  $12^\circ$  and a coarse grid – from  $91^\circ$  to  $60^\circ$ .

The slab was modelled according to the diagram of the free-supported structure distributed along the surface area by the load. The bearing distance of the slab is 2900 mm.

The load was applied for 3 steps. The boundary conditions were applied by means of the Remote Displacement.

The contact between the anchors and the reinforced concrete slab was assigned through Rough – this particular case corresponds to the infinite friction coefficient between the connected bodies; however, with the possible detachment along the surface the absence of friction is implied.

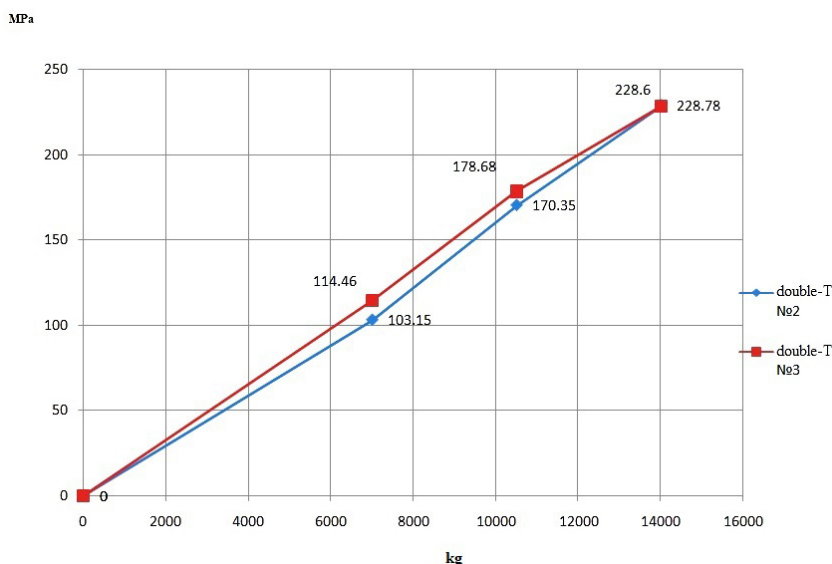


**Figure. 3** Graphs showing the development of loads in the lower flange of the I-beams of a steel reinforced concrete slab

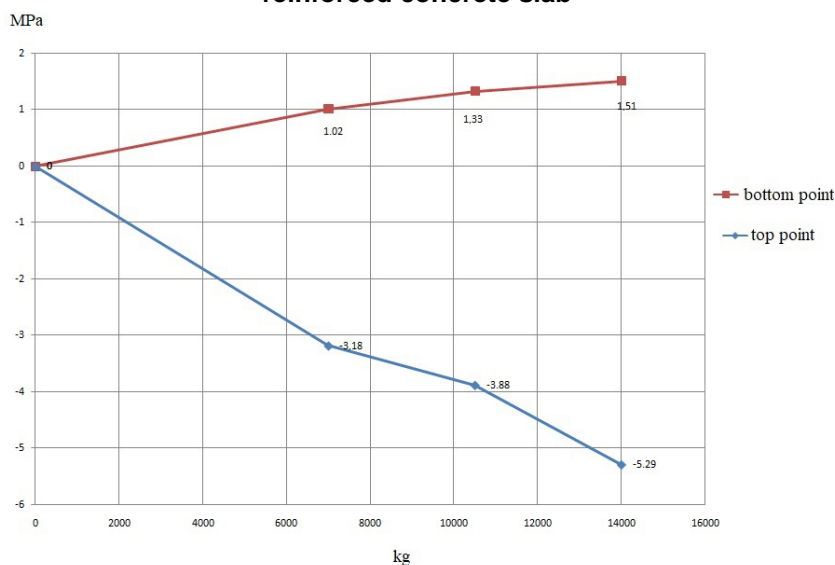


**Figure 4.** Graphs showing the development of loads in a reinforced concrete slab

A calculation of a steel reinforced concrete slab performed on the ANSYS software serves to reveal the situation of a stress-strain state, stages of development of plastic strains in a steel beam and in a concrete slab.

The findings of the studies show a sequence of development of loads and strains in the steel I-beam and in the reinforced concrete slab as strains develop from a more stressed zone to a less stressed one; from the middle to the ends. In a steel beam, strains develop at a more intense pace as the load increases than in a steel reinforced concrete slab which can be explained by a smaller cross-section of the tension flange than a compressed reinforced concrete shelf. Graphs showing the distribution of loads in beams and in a slab

Figures 3–4 and graphs showing changes in deflections (Figure 5) have been formed.

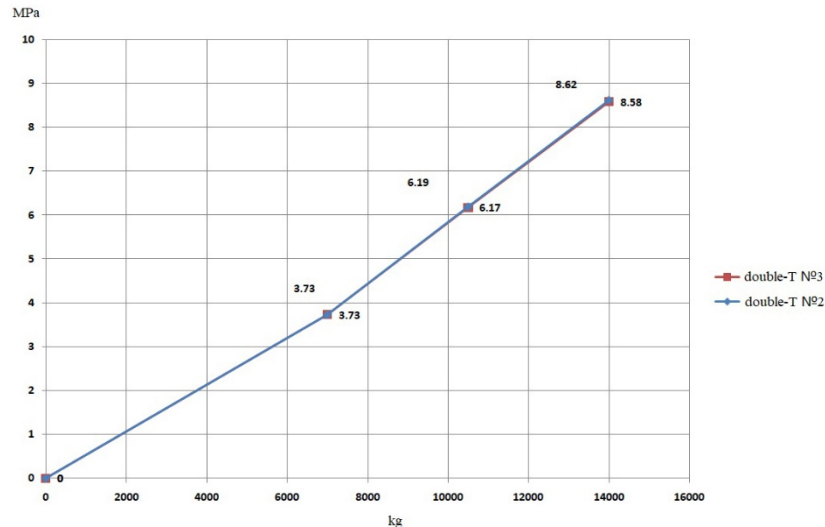


Figure 5. A graph depicting deflections per stage of load

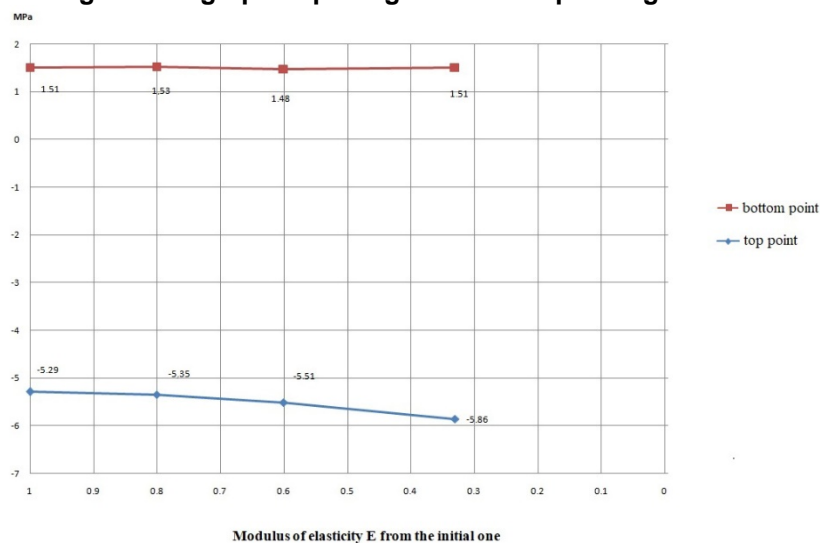


Figure 6. A graph showing the development of loads in the case of a long-term load

Modulus of elasticity E from the initial one.

The attained results of calculations clearly show the development of a stress-strain state in the anchor rods: strains and stresses in them increase as the distance from the middle of a beam grows, stresses increase along the height of rods as they approach the contact zone "steel and concrete"; the surface of the top flange of the steel profile has clearly visible zones of tension using which it is possible to judge about the size of crushed zones or where the concrete in the shelf of a composite beam has split.

The results of the numerical study confirm the theoretical foundation and methodology of calculations of steel reinforced concrete slabs for long-term loads. The creep in the concrete part of the structure confirms the change in the stress-strain state over time. An increase of stresses in the steel part of the structure as the creep accounts for up to 19 %, an increase in deflections up to 39 % in comparison with calculations at short-term loads (Figures 6–8).

To ensure the combined action of metal beams with a slab, various anchoring devices are welded to their upper flange to prevent shifts in the layers. In this study, cylindrical rods have been selected as anchors.

In order to study the peculiarities behind the action of a steel reinforced concrete slab under long-term loads, its large-scale model in the scale 1:2 with the following geometric parameters and components was tested: A reinforced concrete slab with a width of 3 000 mm, a length of 3 000 mm and a height of 45 mm, supported by four steel beams from an I-beam No. 14 GOST (Russian State Standard) 8239-89, with a length of 3 000 mm located at a distance of 1 000 mm from each other. The combined action of steel ribs and the reinforced concrete slab was achieved through two rows of vertical anchor rods (2 $\varnothing$  A400) with a height of 40 mm welded along the entire length to the upper flange of steel I-beams with a step of 150 mm on the ends

at a quarter of the span and with a step of 250 mm in the middle in half span. The concrete slab model was reinforced by reinforcement grids from a wire  $\varnothing 4$  B500 with a step of 200 mm by the classical scheme for ribbed uncut reinforced concrete slabs. The B25-class concrete was used. The slab under the experiment rested against rolling and stationary rollers by means of steel ribs with a working span of 2 900 mm. Rolling and stationary rollers were installed on reinforced concrete blocks on the ends of steel I-beams.

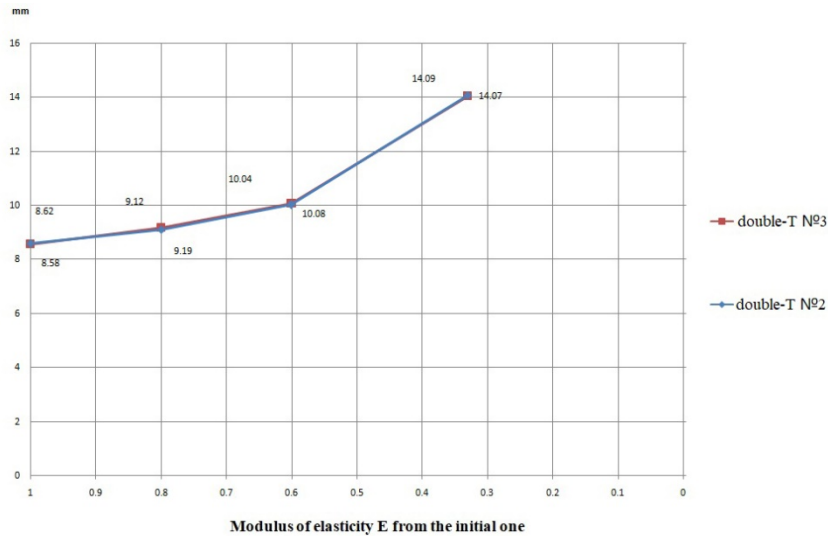


Figure 7. Graphs of the development of deformations in the edges of the plate under prolonged loading

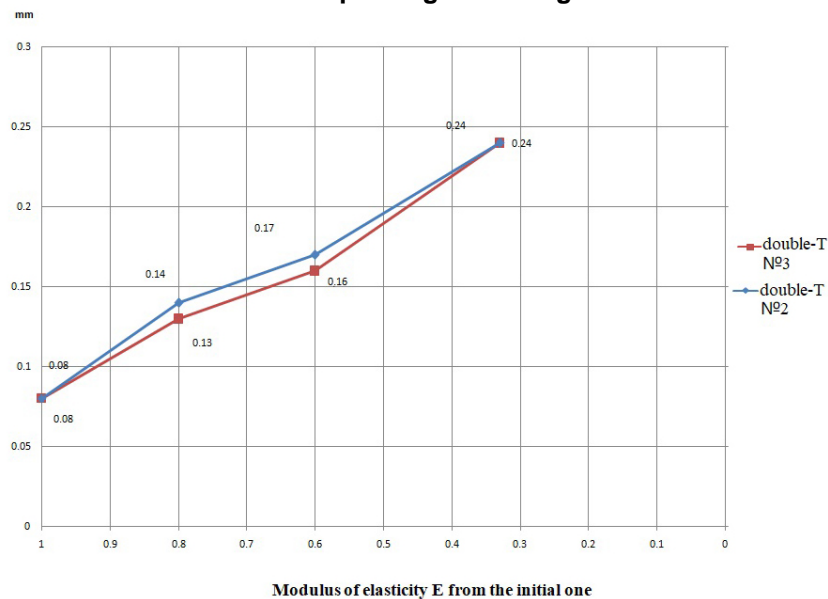


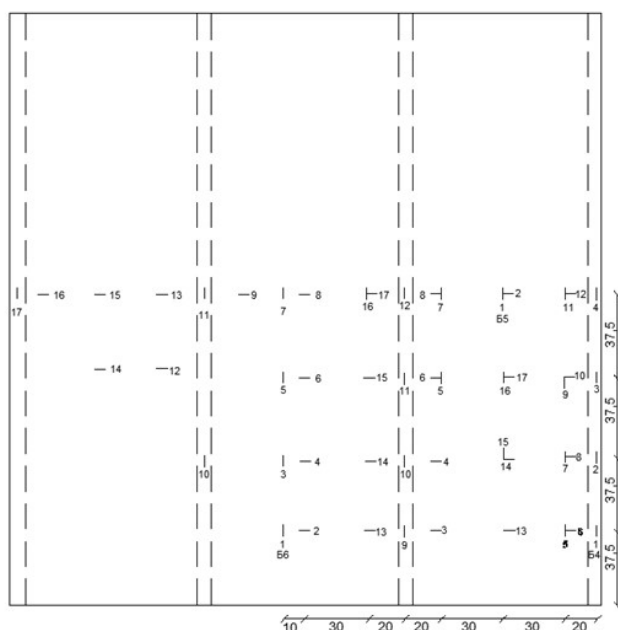
Figure 8. Graph of development of shear at the steel-concrete border



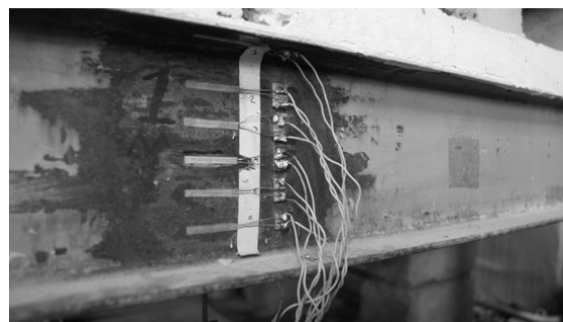
Figure 9. A general view of the slab under load



Figure 10. Dial gauges to record the shift at the border of steel and concrete and settlement of the supports



**Figure 11. A diagram showing the stickers of strain sensors on the bottom surface of the slab**



**Figure 12. Strain sensors on the ribs of the slab**

Vertical strains (deflections) of the slab were measured on the centers of the middle and marginal steel beams by means of beam compasses firmly fixed on a tripod with a dial gage installed under the middle beam. A dial gage (Figure 10) was also installed to measure the settlement of supports in the roller support zone. In order to measure strains (stresses) on the upper and lower surfaces of the concrete slab (Figure 11), resistive-strain sensors with a base of 20 mm (for steel) (Figure 12) and 50 mm (for concrete) were glued onto the walls and shelves of the steel I-beams. A total of 120 resistive-strain sensors were glued. The moment when cracks formed and the manner of their propagation were determined visually; a 24-times magnification MBP-2 microscope was used to measure the values of cracks openings.

The slab fragment model was tested in a laboratory on the premises of the Kazan State University of Architecture and Engineering under static short-term and long-term loads. The static load was transferred to the slab in 48 points in the zone above the steel ribs.

The static evenly distributed load was supplied step-by-step: The distribution layer consisted of 48 reinforced concrete cubes 100 x 100 x 100 in size; the subsequent stages of loads were generated from foundation blocks 400 x 600 x 1200 in size with a weight of 580–590 kg. The second and third layers of the foundation blocks were placed through the wooden gaskets along the ends to provide a static pattern of load transfer from the blocks. A total of 24 blocks were used (Figure 9).

At each stage, the readings of the resistive-strain sensors were taken through AID, deflections in the middle of the beams and the settlement of the supports of the slab were measured and crack formation was observed in the reinforced concrete slab. Strains of the steel ribs were measured as well as those of the I-beams of the reinforced concrete slab and vertical strains of the slab and deflections; based on the readings of resistive-strain sensors and strain indicators, first graphs were formed on the day when the test slab was loaded, i.e. short-term load results. The readings were taken every day during the first week, then once a week. Figures 13–15 show graphs of stress development in the upper and lower flanges of the ribs and in the slab whereas Figure 16 shows a "steel and concrete" shift development at the junction of the ribs with the slab.

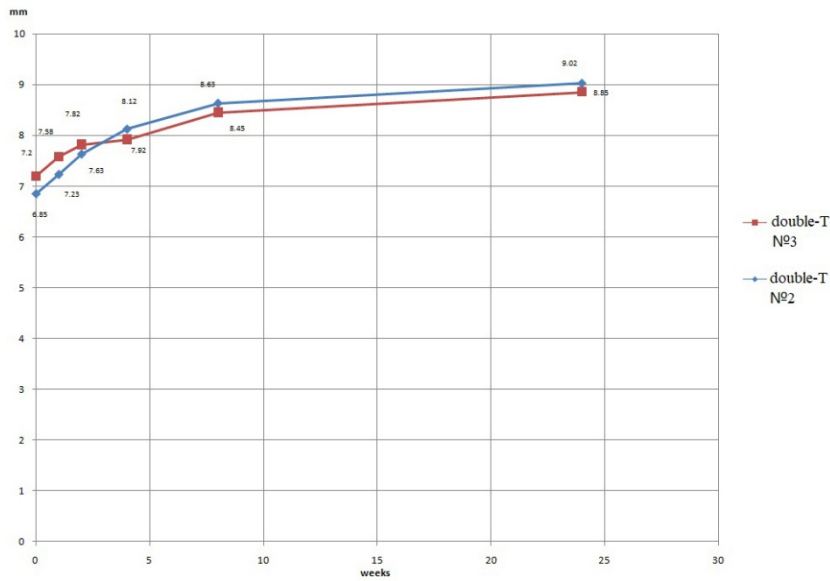


Figure 13. Graphs showing the development of strains in the case of a long-term load

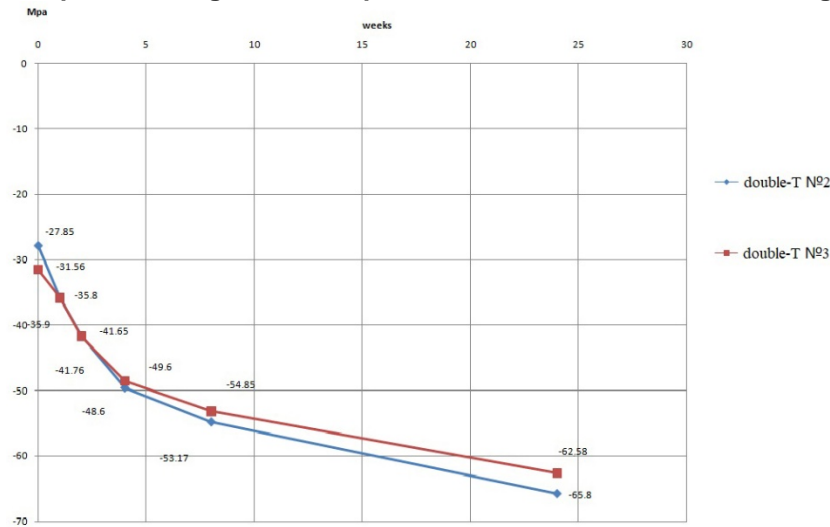


Figure 14. Graphs showing the development of loads in the upper flange of I-beams in the case of a long-term load

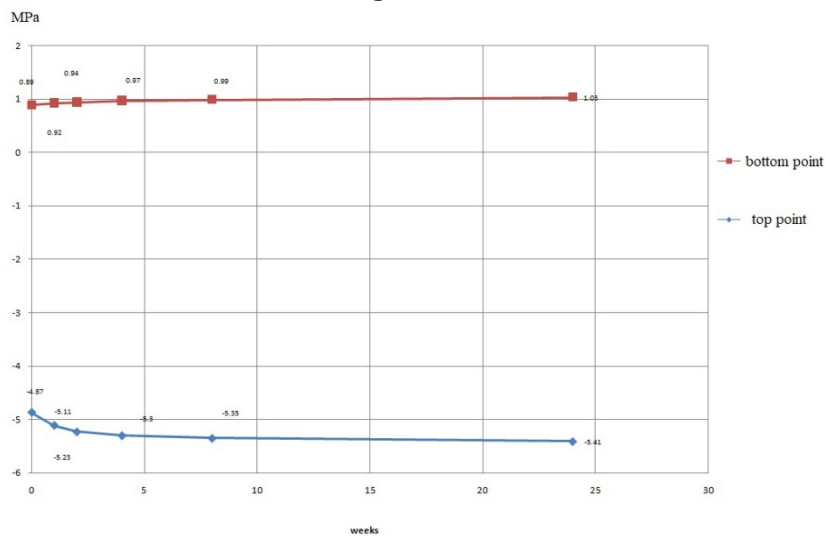
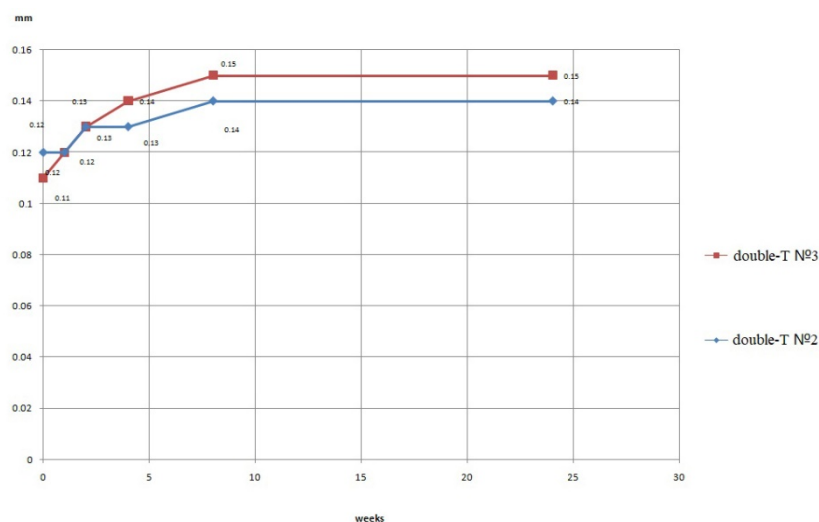


Figure 15. Graphs showing the development of stresses in the case of a long-term load



**Figure 16. Graphs showing the development of a shift at the border of steel and concrete**

An analytical description of the stress-strain state of the steel reinforced concrete slab under long-term loads.

The calculation of the strength of normal cross-sections is performed based on the following prerequisites:

- cross-sections normal to the longitudinal axis of the steel reinforced concrete element are considered;
- normal stresses in the monolithic reinforced concrete slab and a steel beam are taken as calculation data;
- the connection between the main stresses and the relative strains of concrete and steel is presented in the form of corresponding diagrams " $\sigma - \varepsilon$ ".
- the hypothesis of flat cross-sections is considered fair for the average strains of the concrete of the monolithic slab and beams' steel;
- the ductility of the connecting seam (conjunction) of the reinforced concrete part and the steel part of the steel reinforced concrete bending element is not taken into account; the condition of compatibility of strains of concrete and steel along the plane of the contact "steel and concrete" is accepted.

Based on the hypothesis of flat cross-sections and analytical or actual diagrams of concrete " $\sigma_b - \varepsilon_b$ " and steel " $\sigma_s - \varepsilon_s$ " function, the stresses in the concrete of the monolithic slab and in the steel beam are determined by the corresponding strains. Thus, the internal stress forces in the concrete  $\sigma_b$ , in the slab reinforcement  $\sigma_a$  and in the steel of the beam  $\sigma_s$  are defined in the cross-section for any considered load level caused by the action of operational loads.

In this case, there are two equations of equilibrium [1, 2]:

$$N_x = \int_0^{h_n'} \sigma_b[\varepsilon_b(x)] \cdot b_n' \cdot dx + \sigma_s'(\varepsilon_s') \cdot A_s' - \sigma_s(\varepsilon_s) \cdot A_s + \sigma_a'(\varepsilon_a') \cdot A_a' + \sigma_a(\varepsilon_a) \cdot A_a = 0 \quad (1)$$

$$M_z = \int_0^{h_n'} \sigma_b[\varepsilon_b(x)] \cdot b_n' \cdot z_1(x_i) \cdot dx + \sigma_s'(\varepsilon_s') \cdot A_s' \cdot z_2 + \sigma_s(\varepsilon_s) \cdot A_s \cdot z_3 + \sigma_a'(\varepsilon_a') \cdot A_a' \cdot z_4 + \sigma_a(\varepsilon_a) \cdot A_a \cdot z_5 \quad (2)$$

where is " $\sigma_b(\varepsilon_b), \sigma_s'(\varepsilon_s'), \sigma_s(\varepsilon_s), \sigma_a'(\varepsilon_a'), \sigma_a(\varepsilon_a)$ " the dependence of the stress-strain of concrete, steel and reinforcements;

$\varepsilon_b(x)$  – the law of variation of strains along the height of the cross-section of the steel reinforced concrete element;

$b_n'$  – the width of the reinforced concrete monolithic shelf is entered into the calculation;

$x_i$  – the height of the compressed zone;

$z_1$  – the distance from the center of gravity of the curve of normal stresses in monolithic concrete to the neutral axis;

$z_2$  – the distance from the center of gravity of the curve of normal stresses of the compressed part of the steel beam to the neutral axis;

$z_3$  – the distance from the center of gravity of the curve of normal stresses of the stretched area of the steel beam to the neutral axis;

$z_4$  – the distance from the center of gravity of the top reinforcement of the concrete shelf to the neutral axis;

$z_5$  – the distance from the center of gravity of the bottom reinforcement of the concrete shelf to the neutral axis.

Until the condition  $|\Delta N_x| \leq \delta$  ( $\delta$  – the specified accuracy of executions) is fulfilled, the consecutive approximations method is used to calculate the desired height of the compressed zone  $x_i$  of the steel reinforced concrete built-up section according to the formula (1).

For long-term loads, the strength is expressed as

$$M_i + \Delta M_b + \Delta M_{sr} \leq M_z \quad (3)$$

where  $M_i$  is the bending moment of the action of the external load.

$\Delta M_b = 0.5 \left[ \sigma_{b(t)}^{\text{don}} + \sigma_{b(t)}^{\text{don}} \right] b_n h_n z_1 + \sigma_a' A_a' z_4 + \sigma_a A_a z_5$  – an additional bending moment due to the occurrence and accumulation of residual stresses in the concrete of the slab.

$\Delta M_{sr} = \sigma_{sr}'(t) A_{sr}' z_2 + \sigma_{sr}(t) A_{sr} z_3$  – an additional bending moment due to the development of residual stresses in the upper and lower parts of the steel rib's cross-section.

### 3. Discussion

An analysis of the existing literature, rules and regulations pertaining to the design and calculation of steel structures and reinforced concrete structures as well as of instructions and recommendations [12, 13] lead to the conclusion that obtaining theoretical calculations closest to full-scale studies by modeling in the ANSYS software is possible if changes in the stress-strain modulus of the concrete part of the structure and creep are taken into account. Moreover, factors such as temperature, shrinkage and relaxation have less impact on the stress-strain modulus of the structure compared to creep in long-term loads calculations. In this regard, calculations were performed taking into account the changes in the stress-strain modulus of concrete over time taking into consideration the creep coefficient with results attained (A value of  $E_b = 30000$  MPa for concrete B25 was taken as the initial modulus of elasticity). Stresses were also observed which are reflected in the graphs.

The attained results of calculations in ANSYS clearly show the development of a stress-strain state in the anchor rods: strains and stresses in them increase as the distance from the middle of a beam grows, stresses increase along the height of rods as they approach the contact zone "steel and concrete"; the surface of the top flange of the steel profile has clearly visible zones of tension using which it is possible to judge about the size of crushed zones or where the concrete in the shelf of a composite beam has split.

The calculation model used to calculate the durability of normal cross-sections of steel reinforced concrete bending elements is accepted based on analytical diagrams of strains of concrete and steel [1.2]. This approach allows for calculating the structural elements for durability from one position taking into account the non-linear properties of materials at different loads at any moment of time.

– The full-scale tests made it possible to record longitudinal strains of concrete and steel, transverse strains of the concrete of a reinforced concrete slab, strains of the shift at the contact point "steel and concrete" as well as the width of the crack opening and deflections in the structure

– The results of experimental studies allowed for constructing curves of longitudinal and transverse stresses of the steel reinforced concrete slab in the middle zone of the span of the built-up section.

– An analysis of the attained results revealed that due to the creep of concrete caused by long-acting loads in the beams combined with the slab and due to plastic deformations, the share of force endured by the slab goes down which accordingly leads to an additional load on the beam. This said, the greatest additional stress caused by the impact of concrete creep occurs in the top flange of the metal beam connected with the slab by means of anchors.

#### 4. Conclusions

A comparison of the results of stresses according to numerical and full-scale experiments has been made as well as according to analytical formulas.

1) The results of experimental stresses with data obtained by the ANSYS software differ;

– up to 11 % on average for short-term loads.

– up to 19 % for long-term loads.

2) The results of the experiment differ with the analytical method of calculation:

– up to 14 % for long-term loads.

– up to 24 % for long-term loads.

3) The results of the experiment and those of numerical calculations for the shift in the contact plane of steel and concrete presents a good convergence of up to 7 %.

Summarizing the conclusions, it should be noted that numerical methods based on software complexes can be used to investigate the stress-strain state of steel slabs under the action of long loads in the initial period, however, the work material diagrams, changes in their strength properties, must be corrected with experimental data.

For further research, it is necessary to use analytical expressions that most fully reflect the actual work of steel-reinforced concrete structures and to shift them into program complexes in order to accelerate the calculation processes.

#### References

1. Pekin, D. Plitnaya stalezhelezobetonnyaya konstruktsia [Slab steel reinforced concrete structure]. Moscow, 2010. 440 p.
2. Zamaliyev, F. Uchet nelineinikh svoystv materialov i podatlivosti sloev pri raschete prochnosti stalezhelezobetonnykh perekrytiy [Accounting for the non-linear properties of materials and ductility of layers in calculating the durability of steel reinforced concrete floor slabs]. Industrial and civil construction. 2013. No. 5. Pp. 38–41.
3. Zamaliyev, F., Kayumov, R. K raschetu stalezhelezobetonnoy perekrytiya kak ortotropnoy pliti [Calculating a steel reinforced concrete floor slab as an orthotropic bridge]. News of the Kazan State University of Architecture and Engineering. 2014. No. 1(27). Pp. 94–99.
4. Tusnin, A. Perekrytiya mnogoetazhnykh zdaniy so stalnim karkasom [Floor slabs in multi-storied buildings with a steel frame]. Industrial and civil construction. 2015. No. 8. Pp. 10–14.
5. Ayrumyan, E., Kamensikov, N., Rumiyanseva, I. Osobennosti rascheta monolitnykh plit stalezhelezobetonnykh pokritii po profilirovannomu stalnomu nastilu [The peculiarities associated with calculations of monolithic slabs of steel reinforced concrete floor slabs by the steel sheet] // Industrial and civil construction. 2015. No. 9. Pp. 21–26.
6. Tusnin, A., Kolyago, A. Konstruktsia i rabota stalezhelezobetonnoy perekrytiya s ispolzovaniem sbornnykh pustotnykh zhelezobetonnykh plit [Construction and function of steel reinforced concrete floor slabs using precast hollow-core concrete slabs]. Modern science and innovation. 2016. No. 3. Pp. 141–147.
7. Astakhov, I., Kuznetsov, A., Morozova, D. Issledovanie raboti stalezhelezobetonnykh konstruktsii [Studies of the

#### Литература

1. Пекин Д.А. Плитная сталежелезобетонная конструкция. М.: Издательство Ассоциация строительных вузов, 2010. 440 с.
2. Замалиев Ф.С. Учет нелинейных свойств материалов и податливости слоев при расчете прочности сталежелезобетонных перекрытий // Промышленное и гражданское строительство. 2013. № 5. С. 38–41.
3. Замалиев Ф.С., Каюмов Р.А. К расчету сталежелезобетонного перекрытия как ортотропной плиты // Известия КазГАСУ. 2014. № 1(27). С. 94–99.
4. Туснин А.Р. Перекрытия многоэтажных зданий со стальным каркасом // Промышленное и гражданское строительство. 2015. № 8. С. 10–14.
5. Айрумян Э.Л., Каменщиков Н.И., Румянцева И.А. Особенности расчета монолитных плит сталежелезобетонных покрытий по профилированному стальному настилу // Промышленное и гражданское строительство. 2015. № 9. С. 21–26.
6. Туснин А.Р., Коляго А.А. Конструкция и работа сталежелезобетонного перекрытия с использованием сборных пустотных железобетонных плит // Современная наука и инновации. 2016. № 3. С. 141–147.
7. Астахов И.В., Кузнецов А. Ю., Морозова Д. В. Исследование работы сталежелезобетонных конструкций // Вестник гражданских инженеров. 2017. № 3(62)
8. Замалиев Ф.С. Выявление доэксплуатационных напряжений и деформаций стальных балок-ребер сталежелезобетонные перекрытия // Вестник МГСУ. 2013. № 7. С. 33–39
9. Замалиев Ф.С., Биккинин Э.Г. Экспериментальные исследования начального напряженно-деформированного состояния сталежелезобетонных

- function of steel reinforced concrete structures]. The herald of civil engineers. 2017. No. 3(62).
8. Zamaliyev, F. Viyavlenie doekspluatatsionnih napryashenii i deformatsii stalnih stalnih balok-reber stalezhelezobetonnie perekriiya [Identifying the preoperational stresses and strains in steel beam ribs of steel reinforced concrete floor slabs]. The herald of the Moscow State University of Civil Engineering. 2013. No. 7. Pp. 33–39.
  9. Zamaliyev, F., Bikinin, E. Experimentalnih issledovaniya nachalnogo napyashenno-deformirovannogo sostoyania stalezhelezobetonnih balok i plit [Experimental studies of the initial stressed-deformed state of composite steel beams and slabs]. News of the Kazan State University of Architecture and Engineering. 2014. No. 2(32). Pp. 139–143.
  10. Zamaliyev, F., Filippov, V. Raschetno-experimentalnie issledovaniya stalezhelezobetonnih konstruksii [Calculation and experimental studies of composite structures]. Industrial and civil construction. 2015. No. 7. Pp. 29–36.
  11. Zamaliyev, F., Mirsayapov, I. Raschet prochnosti stalezhelezobetonnih izgibaemih konstruksii na osnove analiticheskikh diagramm [A strength calculation of steel reinforced concrete flexible structures based upon analytical programs]. Development and studies of metal and wooden structures: a collection of scientific works. 1999. Pp. 142–149.
  12. BSI (2010) BS 5950-3.1. A1. Structural use of steelwork in buildings. Design in composite construction. Code of practice for design of simple and continuous composite beams. BSI, London.
  13. Roger, P. Jonson Designers' guide to Eurocode 4: design of composite steel and concrete structures EN 1994-1-1. 2011. 412 p.
  14. Vasdravellis, G., Uy, B., Tan, E.L., Kirkland, B. Behaviour and design of composite beams subjected to sagging bending and axial compression Original Research. Journal of Constructional Steel Research. 2015. No. 110. Pp. 29–39.
  15. Hadzalic, E., Barucija, K. Concrete shrinkage effects in composite beam. Construction of Unique Buildings and Structures. 2014. No. 11(26). Pp. 85–93.
  16. Champenoy, D., Corfdir, A., Corfdir, P. Calculating the critical buckling force in compressed bottom flanges of steel-concrete composite bridges. European Journal of Environmental and Civil Engineering. 2014. 18(3). Pp. 271–292.
  17. Gholamhoseini, A., Khanlou, A., MacRae, G., Scott, A., Hicks, S., Leon, R. An experimental study on strength and serviceability of reinforced and steel fibre reinforced concrete (SFRC) continuous composite slabs. Engineering Structures. 2016. 114(1). Pp. 171–180.
  18. Ye, J.H., Chen, W. Elastic restrained distortional buckling of steel-concrete method. International Journal of Structural Stability and Dynamics. 2013. 13(1). Pp. 1–29.
  19. Beck, A.T., DaRosa, E. Structural Reliability Analysis Using Deterministic Finite Element Programs. Latin American Journal of Solids and Structures. 2006. No. 3. Pp. 197–222.
  20. Padmarajaiah, S.K., Ramaswamy, A.A. Finite element assessment of flexural strength of prestressed concrete beams with fiber reinforcement. Cement and Concrete Composites. 2002. No. 24. Pp. 229–241.
  21. Kim, S., Lee, U. Effects of delamination on guided waves in a symmetric laminated composite beam // Mathematical Problems in Engineering. 2014. No. 14. Pp. 12.
  22. Karpov, V.V., Ignat'ev, O.V., Semenov, A.A. The stress-strain state of ribbed shell structures. Magazine of Civil балок и плит // Известия КазГАСУ. 2015. № 2(32). С. 139–143.
  23. Замалиев Ф.С., Филлипов В.В. Расчетно-экспериментальные исследования сталежелезобетонных конструкций // Промышленное и гражданское строительство. 2015. № 7. С. 29–36.
  24. Замалиев Ф.С., Мирсаяпов И.Т. Расчет прочности сталежелезобетонных изгибаемых конструкций на основе аналитических диаграмм // Разработка и исследование металлических и деревянных конструкций: сборник научных трудов. 1999. С. 142–149.
  25. BSI (2010) BS 5950-3.1. A1. Structural use of steelwork in buildings. Design in composite construction. Code of practice for design of simple and continuous composite beams. BSI, London.
  26. Roger P. Jonson Designers' guide to eurocode 4: design of composite steel and concrete structures EN 1994-1-1. 2011. pp. 412.
  27. Vasdravellis G., Uy B., Tan E.L., Kirkland B. Behaviour and design of composite beams subjected to sagging bending and axial compression Original Research // Journal of Constructional Steel Research. 2015. № 110. Pp. 29–39.
  28. Hadzalic E., Barucija K. Concrete shrinkage effects in composite beam// Construction of unique buildings and structures. 2014. № 11(26). Pp. 85–93.
  29. Champenoy D., Corfdir A., Corfdir P. Calculating the critical buckling force in compressed bottom flanges of steel-concrete composite bridges // European Journal of Environmental and Civil Engineering. 2014. № 3(18). Pp. 271–292.
  30. Gholamhoseini A., Khanlou A., MacRae G., Scott A., Hicks S., Leon R. An experimental study on strength and serviceability of reinforced and steel fibre reinforced concrete (SFRC) continuous composite slabs // Engineering Structures. 2016. № 1(114). Pp. 171–180.
  31. Ye J.H., Chen W. Elastic restrained distortional buckling of steel-concrete method // International Journal of Structural Stability and Dynamics. 2013. № 1(13). Pp. 1–29.
  32. Beck A.T., DaRosa E. Structural Reliability Analysis Using Deterministic Finite Element Programs // Latin American Journal of Solids and Structures. 2006. № 3. Pp. 197–222.
  33. Padmarajaiah S.K., Ramaswamy A.A. Finite element assessment of flexural strength of prestressed concrete beams with fiber reinforcement // Cement and Concrete Composites. 2002. № 24. Pp. 229–241.
  34. Kim S., Lee U. Effects of delamination on guided waves in a symmetric laminated composite beam // Mathematical Problems in Engineering. 2014. № 14. Pp. 12.
  35. Карпов В.В., Игнатьев О.В., Семенов А.А. Напряженно-деформированное состояние ребристых оболочечных конструкций // Инженерно-строительный журнал. 2017. № 6(74). С. 147–160.
  36. Назмеева Т.В., Ватин Н.И. Численные исследования сжатых элементов из холодногнутого просечного С-профиля с учетом начальных несовершенств // Инженерно-строительный журнал. 2016. № 2(62). С. 92–101.
  37. Черняев А.А. Вариантное проектирование стальных балочных клеток геометрическими методами// Инженерно-строительный журнал. 2018. № 2(78). С. 3–15.

Engineering. 2017. 74(6). Pp. 147–160.  
doi: 10.18720/MCE.74.12

23. Nazmeeva, T.V., Vatin, N.I. Numerical Investigations of Notched C-Profile Compressed Members with Initial Imperfections. Magazine of Civil Engineering. 2016. 62(2). Pp. 92–101. doi: 10.5862/MCE.62.9
24. Chernyaev A.A. Alternative engineering of steel girder cages by geometrical methods. Magazine of Civil Engineering. 2018. 78(2). Pp. 3–15. doi: 10.18720/MCE.78.1.

*Farit Zamaliev\**,  
+7(987)296-09-49; zamaliev49@mail.ru

*Marat Zakirov*,  
+7(917)294-59-23; z\_marat\_a@mail.ru

*Фарит Сахапович Замалиев\**,  
+7(987)296-09-49;  
эл. почта: zamaliev49@mail.ru

*Марат Азатович Закиров*,  
+7(917)294-59-23;  
эл. почта: z\_marat\_a@mail.ru

© Zamaliev, F.S., Zakirov, M.A., 2018